Review of Palaeobotany and Palynology 298 (2022) 104588

Contents lists available at ScienceDirect

Review of Palaeobotany and Palynology

journal homepage: www.elsevier.com/locate/revpalbo

Leaves of *Taxus* with cuticle micromorphology from the Early Cretaceous of eastern Inner Mongolia, Northeast China

Chong Dong [a,*], Gongle Shi [a], Fabiany Herrera [b], Yongdong Wang [a], Zixi Wang [a], Bole Zhang [c], Xiaohui Xu [d], Patrick S. Herendeen [e], Peter R. Crane [f,g]

[a] State Key Laboratory of Palaeobiology and Stratigraphy, Nanjing Institute of Geology and Palaeontology and Center for Excellence in Life and Paleoenvironment, Chinese Academy of Sciences, Nanjing 210008, China
[b] Earth Sciences, Negaunee Integrative Research Center, Field Museum of Natural History, Chicago, IL 60605, USA
[c] Qingdao Research Institute of Geotechnical Prospecting and Surveying, Qingdao 266030, China
[d] School of Earth and Environment, Anhui University of Science & Technology, Huainan 232001, China
[e] Chicago Botanic Garden, Glencoe, IL 60022, USA
[f] Oak Spring Garden Foundation, Upperville, VA 20184, USA
[g] Yale School of the Environment, Yale University, New Haven, CT 06511, USA

ARTICLE INFO

Article history:
Received 9 November 2021
Received in revised form 11 December 2021
Accepted 14 December 2021
Available online 28 December 2021

Keywords:
Conifers
Taxaceae
Taxus
Early Cretaceous
Huolinhe Basin
Inner Mongolia

ABSTRACT

The Early Cretaceous Huolinhe Formation in eastern Inner Mongolia, northeastern China has yielded abundant and diverse plant fossils, to which we here add a new species of *Taxus* based on exceptionally well-preserved, lignified leaves from the Gucheng open-cast coal mine. *Taxus huolingolensis* sp. nov. has linear leaves with a lamina that tapers to an acute to mucronate apex, and narrows into a decurrent, stalk-like base. The midrib is prominently raised on the abaxial leaf surface. The abaxial leaf cuticle bears dense, short, isodiametric papillae and has two lateral stomatal bands, each of which contains 3–5 short, discontinuous longitudinal rows of stomata. Stomata are longitudinally oriented, amphicyclic, with two polar subsidiary cells and 2–4 lateral subsidiary cells. Each stoma has a more-or-less transversely elongated papillate stomatal ring around the stomatal pit on the outer cuticle surface. *Taxus huolingolensis* sp. nov. closely resembles leaves of extant *Taxus* in gross morphology as well as cuticle micromorphology, and within the genus is most similar to the North American species *T. brevifolia*. Like the leaves of other species of *Taxus* from the Mesozoic, *Taxus huolingolensis* sp. nov. has narrower stomatal bands with fewer stomatal rows in each stomatal band compared to the living species of the genus. The discovery of *T. huolingolensis* adds to our knowledge of Mesozoic Taxaceae and suggests that *Taxus* has been diverse since the Early Cretaceous.

1. Introduction

Taxus L. is one of five small genera in the conifer family Taxaceae, the yew family, that is widely distributed in the northern hemisphere, primarily in temperate regions, and includes about ten extant species of evergreen trees and shrubs (Cope, 1998; Fu et al., 1999a; Eckenwalder, 2009; Wang and Wang and Ran, 2014; Farjon, 2017). Some species (e.g., *Taxus baccata* L.) are widely used in horticulture and the valuable anticancer drug Taxol is extracted and refined from bark and leaves of the yews. *Taxus* is distinguished from other genera of Taxaceae by the helically arranged, linear leaves, and seeds that are partially enclosed by a red fleshy aril with the seed apex remaining exposed (Fu et al., 1999a; Eckenwalder, 2009; Farjon, 2017). *Taxus* is also recognized by its characteristic thick leaf cuticles that have conspicuous, short, isodiametric papillae on the abaxial surface (Ferguson, 1978; Fu et al., 1999a; Ghimire et al., 2014; Elpe et al., 2017; Farjon, 2017).

Molecular phylogenetics resolves *Taxus* as the sister to *Pseudotaxus* W.C. Cheng, with *Austrotaxus* R.H. Compton the sister to these two genera (Leslie et al., 2012; Ran et al., 2018). Together, *Austrotaxus*, *Pseudotaxus*, and *Taxus* comprise the Taxeae, which is sister to the two remaining genera of the family, the clade comprised by *Amentotaxus* Pilger and *Torreya* Arnott. *Cephalotaxus* Siebold & Zuccarini ex Endlicher, which is sometimes included (Price, 2003; Christenhusz et al., 2011) and sometimes excluded (Cheng et al., 2000; Ran et al., 2018) from the family is the sister group to the Taxaceae sensu stricto (Hart, 1987; Price, 1990; Cheng et al., 2000; Leslie et al., 2012; Ran et al., 2018).

The evolutionary history of *Taxus* is poorly known in large part because of its sparse fossil record. Several Mesozoic woods (e.g., *Protelicoxylon*, *Taxaceoxylon*) have anatomical features similar to those of extant Taxaceae, and were probably produced by plants belonging to the family (Philippe et al., 2019). However, except for

* Corresponding author.
E-mail addresses: cdong@nigpas.ac.cn, cdong@nigpas.ac.cn (C. Dong).

https://doi.org/10.1016/j.revpalbo.2021.104588
0034-6667/

Austrotaxus, all extant genera of Taxaceae have very similar wood anatomy (Ghimire et al., 2015) and thus these fossil wood cannot be attributed to specific extant genera.

Jurassic leafy shoots and leaves with well-preserved cuticles that were originally assigned to *Taxus* (Florin, 1958), were later considered to show characters of several extant genera of Taxaceae, and thus cannot be attributed to the extant genus (Harris, 1976). The only reliable fossil occurrence of *Taxus* in the Mesozoic is, *Taxus guyangensis* X.H. Xu et B.N. Sun, a leafy shoot with attached seed-bearing structures from the Early Cretaceous of Inner Mongolia, China (Xu et al., 2015). In this paper, we add to the Early Cretaceous fossil record of *Taxus* and describe a new species based on exceptionally well-preserved, lignified leaves from the Early Cretaceous Huolinhe Formation in eastern Inner Mongolia, northeastern China. Fossil leaves of *Taxus huolingolensis* sp. nov. are the most informative fossil leaves attributed to *Taxus* so far from the Mesozoic and contribute new information for understanding the diversity and evolution of this genus, as well as the Taxaceae more broadly, during the later Mesozoic.

2. Material and methods

2.1. Geological setting

The fossil leaves described in this study are all from sediment sample (PSH344) collected at the Gucheng open-cast coal mine (45°32′28.9″ N, 119°35′49″ E) in Huolin Gol, eastern Inner Mongolia Autonomous Region, northeastern China (Fig. 1), during a Sino-US joint field expedition in July, 2017 (Shi et al., 2021a, 2021b). The lignitic mudstone that yielded the fossil leaves belongs to the Huolinhe Formation, which is deposited in the Huolinhe Basin, and is one of the largest of the several coal-bearing sedimentary basins in northern China that formed during the Late Jurassic and Early Cretaceous (Li et al., 1982; Deng, 1995).

The Huolinhe Formation comprises a sequence of terrestrial and fluvio-lacustrine-swamp deposits up to 1700 m thick and unconformably overlays the Upper Jurassic Xing'anling Volcanic Group (Deng, 1995). The Huolinhe Formation is subdivided into six members based on lithology. In ascending order they are: "sandy conglomerate member", "lower mudstone member", "lower coal-bearing member", "upper mudstone member", "upper coal-bearing member", and "top mudstone member" (Deng, 1995). Exploitable coals and lignites occur mainly in the lower coal-bearing member, which is ca. 720 m thick and yields abundant, well-preserved compression plant fossils (Sun, 1987, 1993; Sun and Shang, 1988; Chen and Deng, 1990; Deng, 1991, 1995; Sun et al., 2003; Dong and Sun, 2012; Xu et al., 2013, 2017; Guignard et al., 2019) and silicified petrifactions (Matsunaga et al., 2021; Shi et al., 2021a; Herrera et al., 2022). U–Pb zircon geochronology of an ash layer near the bottom of the "lower coal-bearing member" in the nearby Zhahanaoer open-cast coal mine gave an age of 125.6 ± 1.0 Ma (late Barremian–earliest Aptian), consistent with age estimates based on palynological assemblages from the "lower coal-bearing

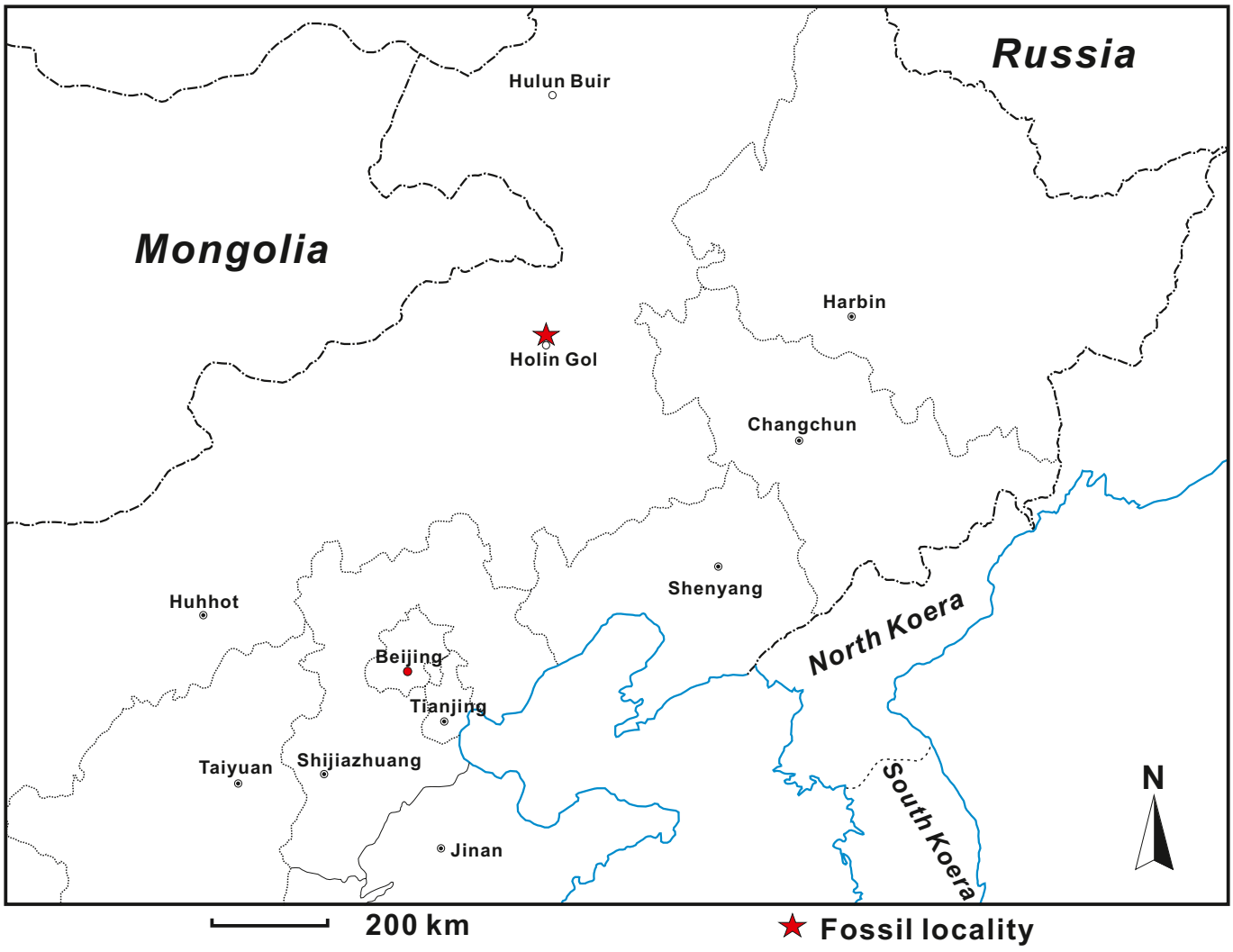

Fig. 1. Map showing location of the Gucheng open-cast coal mine (45°32′28.9″ N, 119°35′49″ E) in Huolin Gol, eastern Inner Mongolia Autonomous Region, northeastern China.

member" (Guo, 1995; Shi et al., 2021b). Boreholes and stratigraphic analyses suggest the deposit in Gucheng coal mine that yielded the fossils described in this paper belongs to the "lower coal-bearing member" and is above the ash layer in Zhahanaoer open-cast coal mine that yielded the U–Pb dates. No significant stratigraphic unconformities have been observed in the sequence. We therefore consider the age of the studied fossil leaves as late Barremian–early Aptian. The fossil plant assemblage from the "lower coal-bearing member" of the Huolinhe Formation is diverse, and consists of bryophytes, lichens, lycopods, horsetails, ferns, and a variety of seed plants, including angiophytes, cycads, conifers, and ginkgophytes, as well as seeds and cones of uncertain affinity (Deng, 1995; Matsunaga et al., 2021; Shi et al., 2021a; Herrera et al., 2022).

2.2. Preparation of the fossil and extant material

The fossil leaves were picked from the surface of the sediment using fine-tipped forceps under a stereo microscope, cleaned with dilute hydrochloric acid for two to three hours, followed by hydrofluoric acid (50%) for 12 h, then thoroughly washed in distilled water. Isolated fossil leaves were cleaned manually using a small brush and forceps to remove adhering small organic matter and then dried in air. Selected specimens were mounted on microscope slides with glycerin and observed and photographed using a Leica M205A stereomicroscope equipped with a Leica DFC450 digital camera system at the Nanjing Institute of Geology and Palaeontology, Chinese Academy of Sciences (NIGPAS).

Leaf cuticles were obtained by maceration in Schulze's solution (HNO_3 catalyzed with $KClO_3$) for approximately 4–6 h. The macerated leaves were washed thoroughly in distilled water and treated with NH_4OH (5%) for a few minutes until the upper and lower cuticles were completely separated. Isolated cuticles were washed thoroughly again in distilled water and mounted on slides with glycerin jelly. The cuticle slides were examined and photographed with differential inference contrast illumination using an Olympus BX53 microscope equipped with an Olympus DP73 camera at NIGPAS. Cuticles for scanning electron microscope (SEM) examination were then dehydrated in a series of 50%, 75%, 90%, and 100% EtOH, mounted on stubs with conductive tape, dried in air, coated with gold, and observed and photographed using a TESCAN MAIA 3 GMU and a SU3500 at NIGPAS.

Leaves and shoot fragments of extant *Taxus brevifolia* Nutt., *T. floridana* Nutt. ex Chapm., and *T. wallichiana* Zucc. used for comparison are from the Herbarium of Institute of Botany, Jiangsu Province and Chinese Academy of Sciences (with the prefix 'NAS'); and leaves and shoot fragments of *T. chinensis* (Pilg.) Rehd. and *T. mairei* (Lemée & Lév.) S.Y. Hu ex T.S. Liu were collected from living trees at the Shanghai Chenshan Botanical Garden (Chenshan). The middle sections of the leaves were cut and processed in a mixture of 10% acetic acid and 10% hydrogen peroxide (1:1) and heated in a water bath at 80 °C for approximately 12 h until leaf fragments turned white and semitransparent. After thoroughly washing in distilled water, the upper and lower leaf cuticles were separated using a dissecting needle and remaining cellular material was removed with a small brush. Cuticle slides and SEM stubs of extant *Taxus* leaves were prepared using the same method as the fossil cuticles.

The studied specimens, including cuticle slides and SEM stubs, are deposited in the Palaeobotanical Collections of the Nanjing Institute of Geology and Palaeontology, Chinese Academy of Sciences. The terminology for the description of the stomata and papillae of *Taxus* follows Elpe et al. (2017).

3. Systematic paleobotany

Order: Coniferales Gorozhankin
Family: Taxaceae Grey

Genus: **Taxus** L.

Species: *Taxus huolingolensis* Dong, Shi, Herrera, Wang, Wang, Zhang, Xu, Herendeen, et Crane, sp. nov. (Plate I, 1–8, Plate II, 1–5, Plate III, 1–7, Plate IV, 1–10, Plate V, 1–7, Plate VI, 1–6, Plate VII, 1–9).

Etymology: The specific epithet derives from the city of Huolin Gol, where the fossil locality belongs to.

Locality: The Gucheng open-cast coal mine (45°32′28.9″ N, 119°35′49″ E), Huolin Gol, eastern Inner Mongolia Autonomous Region, northeastern China.

Holotype: PB23811 (Plate I, 1, Plate III, 6)

Other illustrated material: PB23812 (Plate I, 3), PB23813 (Plate I, 2), PB23814 (Plate I, 7), PB23816 (Plate I, 8, Plate III, 1, 3), PB23817 (Plate I, 6), PB23818 (Plate I, 5), PB23820 (Plate I, 4), PB23844 (Plate III, 4, 5), PB23845 (Plate III, 2), PB23847 (Plate II, 5), PB23848 (Plate II, 1), PB23851 (Plate II, 2), PB23853 (Plate II, 3), PB23855 (Plate II, 4), PB23862 (Plate V, 3), PB23863 (Plate III, 7, Plate V, 4), PB23864 (Plate V, 1), PB23866 (Plate V, 2, 5–7), PB23867 (Plate IV, 7–10, Plates VI, 1–6, VII, 1–9), PB23870 (Plate IV, 2), PB23871 (Plate IV, 1), PB23872 (Plate IV, 3), PB23876 (Plate IV, 5), PB23877 (Plate IV, 6), PB23879 (Plate IV, 4).

Additional studied material: PB23815, PB23819, PB23821, PB23822, PB23823, PB23824, PB23825, PB23826, PB23827, PB23828, PB23829, PB23830, PB23831, PB23832, PB23833, PB23834, PB23835, PB23836, PB23837, PB23842, PB23843, PB23846, PB23849, PB23850, PB23852, PB23854, PB23856, PB23857, PB23858, PB23859, PB23860, PB23861, PB23865, PB23868, PB23869, PB23873, PB23874, PB23875, PB23878.

Stratigraphic horizon and age: The Huolinhe Formation, Late Barremian–early Aptian, Early Cretaceous.

Diagnosis: Leaves borne helically. Leaves linear, straight, to slightly curved near the narrowed base. Leaf apex acute to mucronate and leaf margin entire. Midrib raised on abaxial leaf surface. Stomata in two bands on abaxial leaf surface. Adaxial cuticle with rectangular epidermal cells regularly arranged in longitudinal files, with straight anticlinal walls and smooth periclinal walls. Abaxial cuticle covered with dense papillae except near the leaf margins. Papillate zone of the leaf with two well-defined stomatal bands as well as two sub-marginal zones and midrib that lack stomata. Epidermal cells in the papillate zone rectangular with straight anticlinal walls and arranged in regular longitudinal files; each bearing 2–6 (commonly 3–4) short, isodiametric papillae on their periclinal walls. Stomata in in each stomatal band longitudinally oriented, arranged in 3–5 short, discontinuous longitudinal rows. Stomatal complexes amphicyclic, two guard cells surrounded by two polar subsidiary cells and 2–4 lateral subsidiary cells. Subsidiary cells bearing papillae on the outer cuticle surface that are somewhat fused to form a transversely elongated stomatal ring.

Description: Taxus huolingolensis sp. nov. is known mainly from detached leaves (Plate I, 1–8), and a few fragments of leafy shoots bearing only decurrent leaf bases (Plate II, 1–5, Plate IV, 1, 2). The holotype (Plate I, 1) is a complete isolated linear leaf, 11.6 mm long and 1.5 mm wide. The leaf has an acute apex, a slightly curved and narrowed base, and a prominent midrib raised on the abaxial surface. The leafy shoots and leaves are considered to belong to the same species based on similarities in their cuticular structures. Axes of the leafy shoots are 1.2–1.6 mm wide, and the persistent leaf bases attached to the axes are ca. 0.4–0.7 mm in diameter (Plate II, 1–5, Plate IV, 1, 2). Where they attach to the shoots the leaf bases are narrow, decurrent, and inserted helically and densely.

Leaves are coriaceous and thick, yellow or brown in color, and are preserved as more-or-less translucent compressions (Plate I, 1–8, Plate III, 1–6). Leaf blades are dorsi-ventrally flattened, linear, straight and bilaterally symmetrical or sometimes slightly curved near the base. Leaves are ca. 10.0–20.0 mm long (typically 12–16 mm) and ca. 1.2–2.0 mm wide, with a length/width ratio of 6.7–10.5 (Plate I, 1–8). The widest part of the leaf is near the middle or slightly toward the base (Plate I, 1–4, 7, 8). The leaf apex is acute to mucronate. At the base the leaves are sessile and the lamina is narrowed and stalk-like (Plate I, 1–4, 7,

Plate I. *Taxus huolingolensis* sp. nov. (**1–8**) and leaves of selected extant species of *Taxus* (**9–18**) for comparison. **1–8.** *Taxus huolingolensis* sp. nov., fossil leaves showing variation in form and size. **1.** Holotype, PB23811. **2.** PB23813. **3.** PB23812. **4.** PB23820. **5.** PB23818. **6.** PB23817. **7.** PB23814. **8.** PB23816. **9, 10.** *Taxus chinensis* (Pilg.) Rehd. Tree no. 030251 (Chenshan). **11, 12.** *Taxus mairei* (Lemée & Lév.) S.Y. Hu ex T.S. Liu. Tree no. 102580 (Chenshan). **13, 14.** *Taxus wallichiana* Zucc. NAS00166100. **15, 16.** *Taxus floridana* Nutt. ex Champ. NAS00166214. **17, 18.** *Taxus brevifolia* Nutt. NAS00166219. Scale bar = 2 mm.

8). Leaf margins are entire (Plate I, 1–8, Plate III, 1–6, Plate IV, 3–6). Adaxial and abaxial leaf surfaces are easily distinguished by the dense covering of prominent papillae of the abaxial surface that are clearly visible under the microscope. The midrib is ca. 0.1–0.3 mm wide, continuous from base to apex, and is generally raised on abaxial leaf surface (Plate I, 1–6, Plate III, 1, 4, 5). On the adaxial leaf surface the midrib is not prominently raised but is conspicuous due to its slightly darker color (Plate I, 7, 8). Resin bodies or resin canals have not been observed in any of the leaves (Plate I, 1–8). Small dark spots on the leaf surface are common and likely represent remains of fungal stromata (Plate I, 1, 2).

Cuticles are thick and well preserved with stomata present only on the abaxial surface (Plate III, 7, Plate IV, 7–8). Adaxial epidermal cell outlines are rectangular in outline, slightly elongated along the long axis of the leaf, often with oblique end walls. They are 35–80 μm (commonly 40–60 μm) long, 20–35 μm (commonly 20–30 μm) wide, with a length/width ratio of ca. 1.15–4.30 (Plate V, 1, Plate VI, 1, 2), and are

Plate II. *Taxus huolingolensis* sp. nov. (**1–5**) and leafy shoots of selected extant species of *Taxus* (**6–8**) for comparison. **1–5.** *Taxus huolingolensis* sp. nov., shoot fragments with attached leaf bases. **1.** PB23848. **2.** Shoot fragment and line drawing showing helical arrangement of leaf bases. PB23851. **3.** PB23853. **4.** PB23855. **5.** Shoot fragment and line drawing showing attached decurrent and helically inserted leaf bases. PB23847. **6.** *T. brevifolia* Nutt. NAS00166219. **7.** *Taxus chinensis* (Pilg.) Rehd. Tree no. 030251 (Chenshan). **8.** *Taxus mairei* (Lemée & Lév.) S. Y. Hu ex T. S. Liu. Tree number. 102580. Scale bar = 2 mm.

regularly arranged in longitudinal files. Epidermal cell outlines over the midrib and marginal zones are generally similar to those on other parts of the adaxial surface but the cells are somewhat more elongated, with a length/width ratio up to ca. 2.2–5.0 (Plate IV, 9, 10, Plate VI, 1, 2). Anticlinal walls of the epidermal cell outlines on the adaxial surface are straight, ca. 1.6–2.1 μm thick, with well-developed anticlinal cuticular walls (Plate VI, 1, 2) that are slightly thicker over the midrib and near the leaf margins (Plate VI, 1, 2). The inner (Plate VI, 1, 2) and outer (Plate IV, 9) cuticular periclinal surfaces are generally smooth at high magnification using SEM. They lack cuticular thickenings or papillae (Plate IV, 9, 10), and are finely mottled under LM (Plate V, 1).

The abaxial epidermis bears dense, conspicuous papillae except near the leaf margins and on the decurrent base (Plate III, 7, Plate IV, 7). The papillae are densely and evenly distributed from leaf base to apex, but are nearly absent at the base. The non-papillate regions near the leaf margins are almost equal in width (ca. 140–190 μm wide) and are composed of 6–9 files of longitudinally oriented epidermal cell outlines (Plate III, 7, Plate IV, 8) that are 55–118 μm long and 16–32 μm wide, with a length/width ratio of ca. 2.0–7.3 (Plate V, 3, Plate VI, 5). Anticlinal walls of the cell outlines are straight, well-developed, ca. 2.4 μm in thickness (Plate VI, 5); the periclinal walls are generally smooth (Plate VI, 3, 5).

The broad papillate zone includes two lateral stomatal bands separated by a midrib zone that lacks stomata, and two narrow non-stomatal sub-marginal zones from which stomata are also absent (Plate III, 7, Plate IV, 7). In the papillate zone each epidermal cell bears 2–6 (commonly 3–4) short, isodiametric papillae on the periclinal walls (Plate V, 2–7, Plate VI, 3, 4). Externally the papillae are 8.0–12.0 μm in diameter, and sometimes several papillae are more-or-less fused longitudinally (Plate VI, 3, 4, Plate VII, 1–3).

The non-stomatal zone over the midrib is approximately 350–420 μm wide (Plate III, 7, Plate IV, 7, 8, Plate VI, 4, 6), and the sub-marginal zone that also lacks stomata is ca. 140–180 μm wide (Plate III, 7, Plate IV, 7, 8, Plate VI, 4, 5). Epidermal cell outlines over the non-stomatal midrib and sub-marginal zones are similar in form and are usually rectangular, often with oblique end walls. They are arranged in longitudinal files, with straight anticlinal walls and well-developed cuticular flanges (Plate IV, 8, Plate VI, 5, 6). The cell outlines are 30–90 μm (commonly 45–65 μm) long and 16–30 μm (commonly 20–25 μm) wide, with a length/width ratio of ca. 1.3–3.0 (Plate V, 3, 4, Plate VI, 5, 6). The inner surface of the cuticle in the non-stomatal midrib zone is almost smooth, suggesting that the papillae on the outer surface are solid (Plate VII, 9). In the non-stomatal zones near the leaf margin

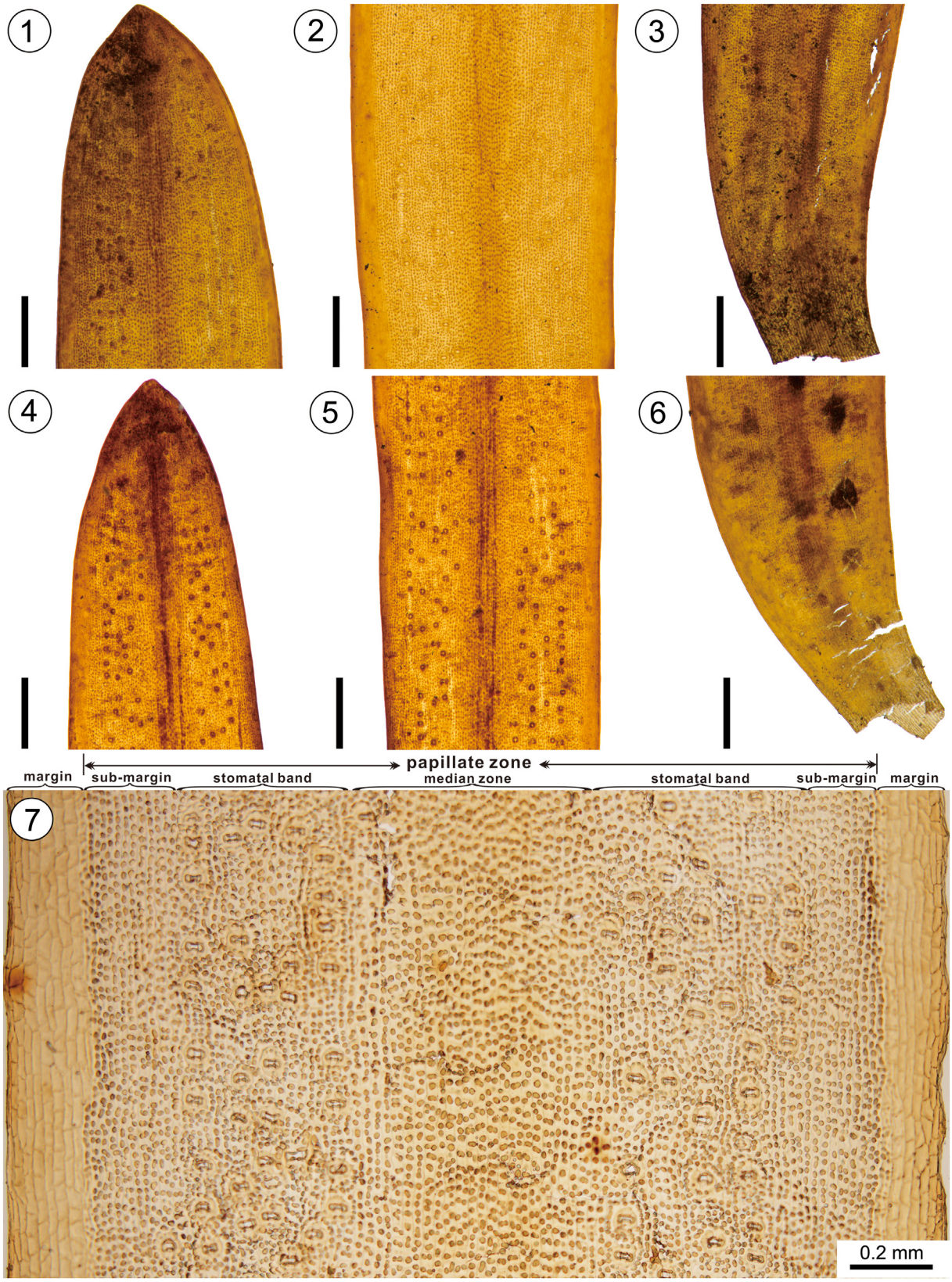

Plate III. *Taxus huolingolensis* sp. nov., light micrographs of leaves and abaxial cuticles. **1.** Detail of apex of leaf in Plate I, 8 showing acute apex, and dense, prominent papillae on the abaxial surface. PB23816. **2.** Detail of middle portion of leaf blade showing broad papillate zone with two lateral non-papillate zones. PB23845. **3.** Detail of basal portion of leaf blade in Plate I, 8 showing narrowing toward the stalk-like leaf base. PB23816. **4.** Detail of leaf apex showing acute apex and prominent midrib; note two well-developed lateral stomatal bands with irregular discontinuous longitudinal rows of stomata and the broad papillate zone extending across almost the entire width of the leaf. PB23844. **5.** Detail of middle portion of leaf blade showing broad papillate zone including two lateral stomatal bands, each with 4–5 irregular longitudinal rows of stomata; note the prominent midrib. PB23844. **6.** Detail of basal portion of leaf in Plate I, 1 showing narrowing toward the stalk-like leaf base. PB23811. **7.** Abaxial cuticle in middle part of leaf blade across the full leaf width showing two non-papillate zones along the leaf margin, and the broad papillate zone that is composed of a median midrib zone, two lateral stomatal bands and two sub-marginal zones. PB23863. Scale bars: **1–6** = 500 μm; **7** = 200 μm.

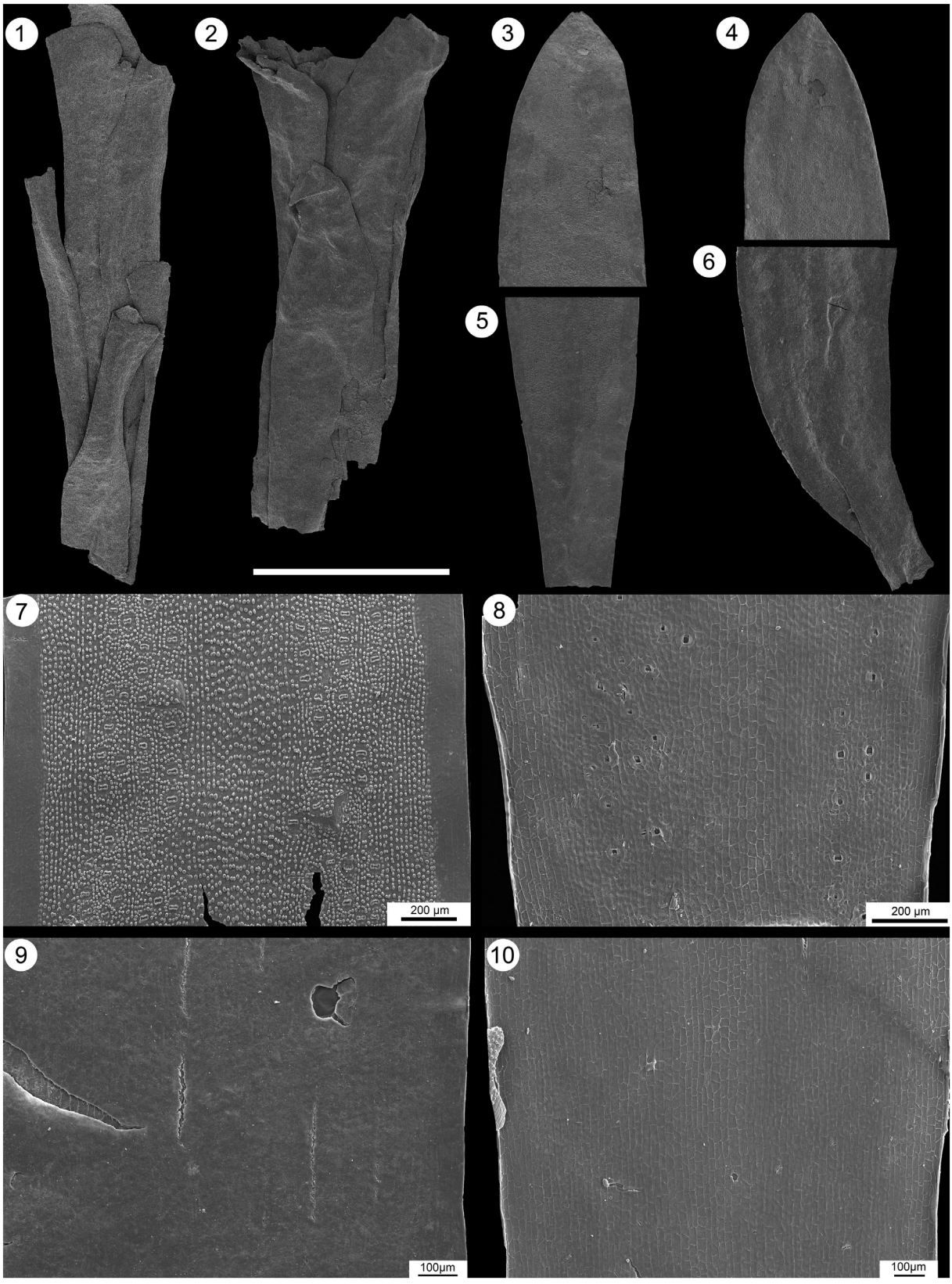

Plate IV. *Taxus huolingolensis* sp. nov., scanning electron micrographs of shoot fragment, leaves and leaf cuticles. **1, 2.** shoot fragments showing helically arranged, decurrent stalk-like leaf bases. **1.** PB23871. **2.** PB23870. **3, 4.** Detail of leaf apices showing an acute and mucronate apex. **3.** PB23872. **4.** PB23879. **5, 6.** Detail of lower part of leaf lamina showing narrowing toward the stalk-like leaf base. **5.** PB23876. **6.** PB23877. **7.** Outer surface of abaxial cuticle in middle part of leaf across the full leaf width showing two non-papillate marginal zones and broad papillate zone consisting of a median midrib zone, two lateral stomatal bands and two non-stomatal sub-marginal zones. PB23867. **8.** Inner surface of abaxial cuticle near basal part of leaf across the full leaf width showing epidermal cells and stomatal complexes in irregular longitudinal rows in the two lateral stomatal bands. PB23867. **9.** Outer surface of adaxial cuticle in middle part of leaf showing the smooth surface. PB23867. **10.** Inner surface of adaxial cuticle in middle part of leaf across the full leaf width showing rectangular epidermal cell outlines arranged in longitudinal files oriented parallel along the long axis of the leaf. PB23867. Scale bars: **1–6** = 1.0 mm; **7, 8** = 200 μm; **9, 10** = 100 μm.

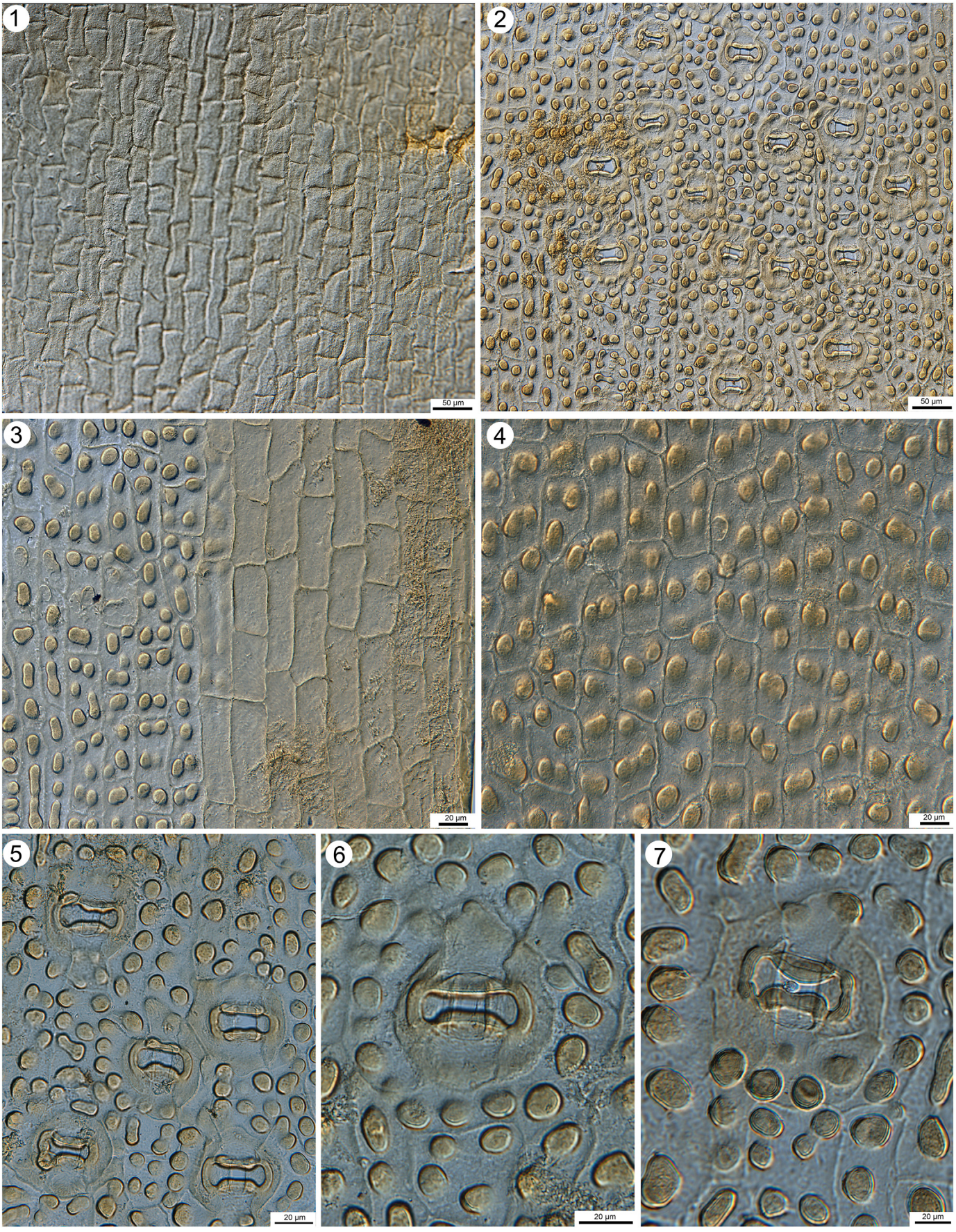

Plate V. *Taxus huolingolensis* sp. nov., light micrographs of leaf cuticles. **1.** Adaxial cuticle showing rectangular epidermal cell outlines arranged in longitudinal files. PB23864. **2.** Abaxial cuticle showing outlines of papillate epidermal cells and stomatal complexes in irregular discontinuous longitudinal rows in the stomatal band. PB23866. **3.** Abaxial cuticle near leaf margin showing epidermal cell outlines in non-papillate marginal zone, and cell outlines with papillae in the sub-marginal portion of the papillate zone. PB23862. **4.** Abaxial cuticle from non-stomatal median zone over the midrib showing epidermal cell outlines and isodiametric papillae. PB23863. **5.** Abaxial cuticle showing five stomatal complexes with transversely elongated papillate stomatal rings surrounding the stomatal pit. PB23866. **6, 7.** Abaxial cuticle showing details of stomata on outer cuticle surface with transversely elongated papillate stomatal rings. PB23866. Scale bars: **1, 2** = 50 μm; **3–7** = 20 μm.

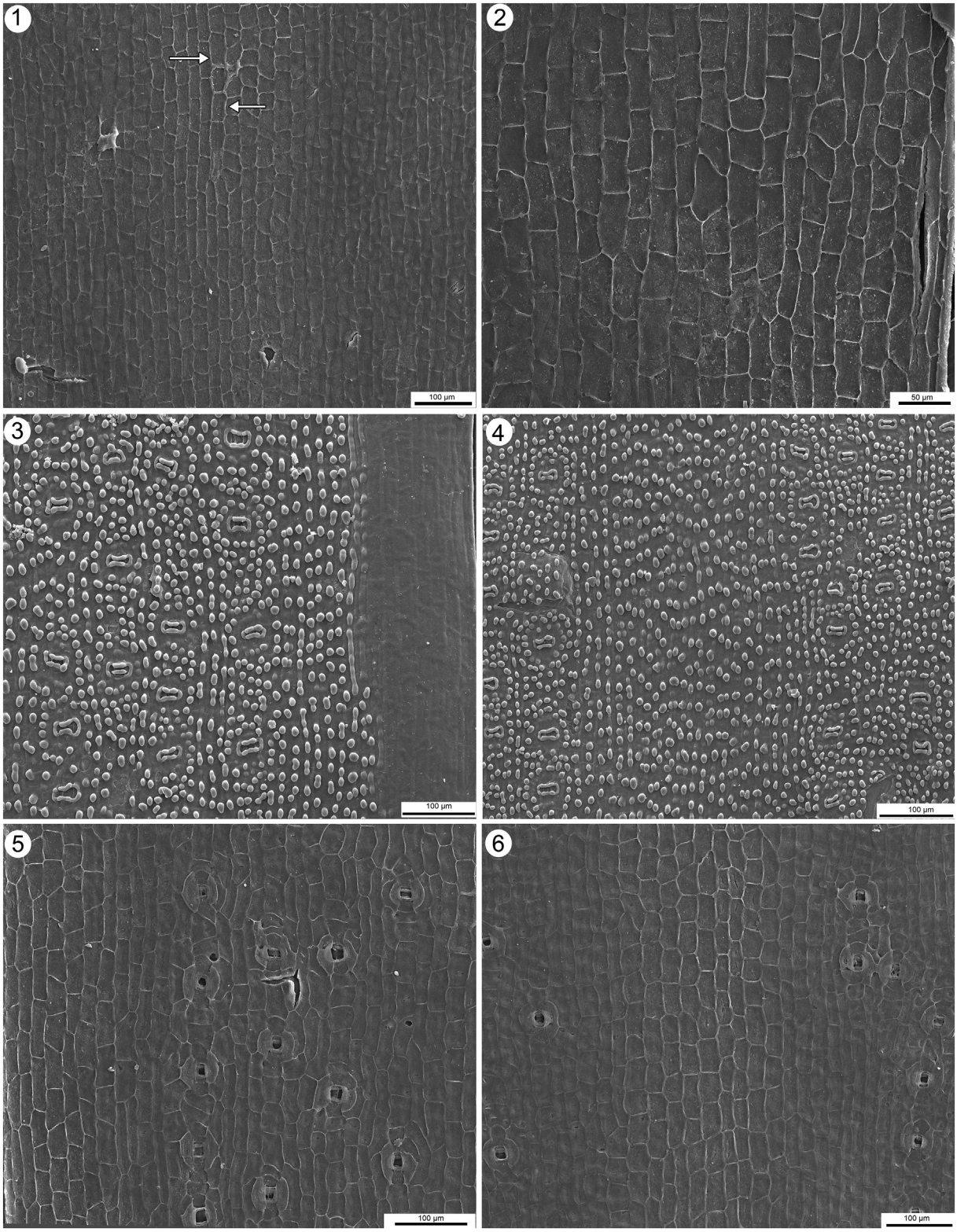

Plate VI. *Taxus huolingolensis* sp. nov., scanning electron micrographs of cuticles from a single fossil leaf. PB23867. **1.** Adaxial cuticle from the middle region of leaf showing rectangular epidermal cell outlines arranged in longitudinal files; note the anticlinal flanges of cells over the midrib (arrows) are slightly thicker than those over the rest of the leaf. **2.** Adaxial cuticle near leaf margin showing rectangular epidermal cell outlines arranged in longitudinal files; note that many cells are elongated and most have well developed anticlinal flanges. **3.** Abaxial cuticle outer surface showing non-papillate epidermal cells near the leaf margin, and short, isodiametric papillae on epidermal cells in the sub-marginal zone and the stomatal band. **4.** Abaxial cuticle outer surface of the non-stomatal midrib zone and flanking stomatal bands, showing isodiametric papillae on the epidermal cells, and stomatal complexes arranged in irregular discontinuous longitudinal rows, each with a transversely elongated papillate stomatal ring. **5.** Abaxial cuticle inner surface over the marginal zone, sub-marginal zone and stomatal band showing elongated epidermal cell outlines and stomata longitudinally arranged in irregular discontinuous longitudinal rows; note epidermal cell outlines near the margin are longer and with thicker anticlinal flanges. **6.** Abaxial cuticle inner surface over the stomatal bands and non-stomatal midrib zone showing elongated epidermal cell outlines and stomata arranged in irregular discontinuous longitudinal rows; note rectangular epidermal cells in the non-stomatal midrib zone are longer and with thicker anticlinal flanges. Scale bars: **1, 3, 4, 5, 6** = 100 μm; **2** = 50 μm.

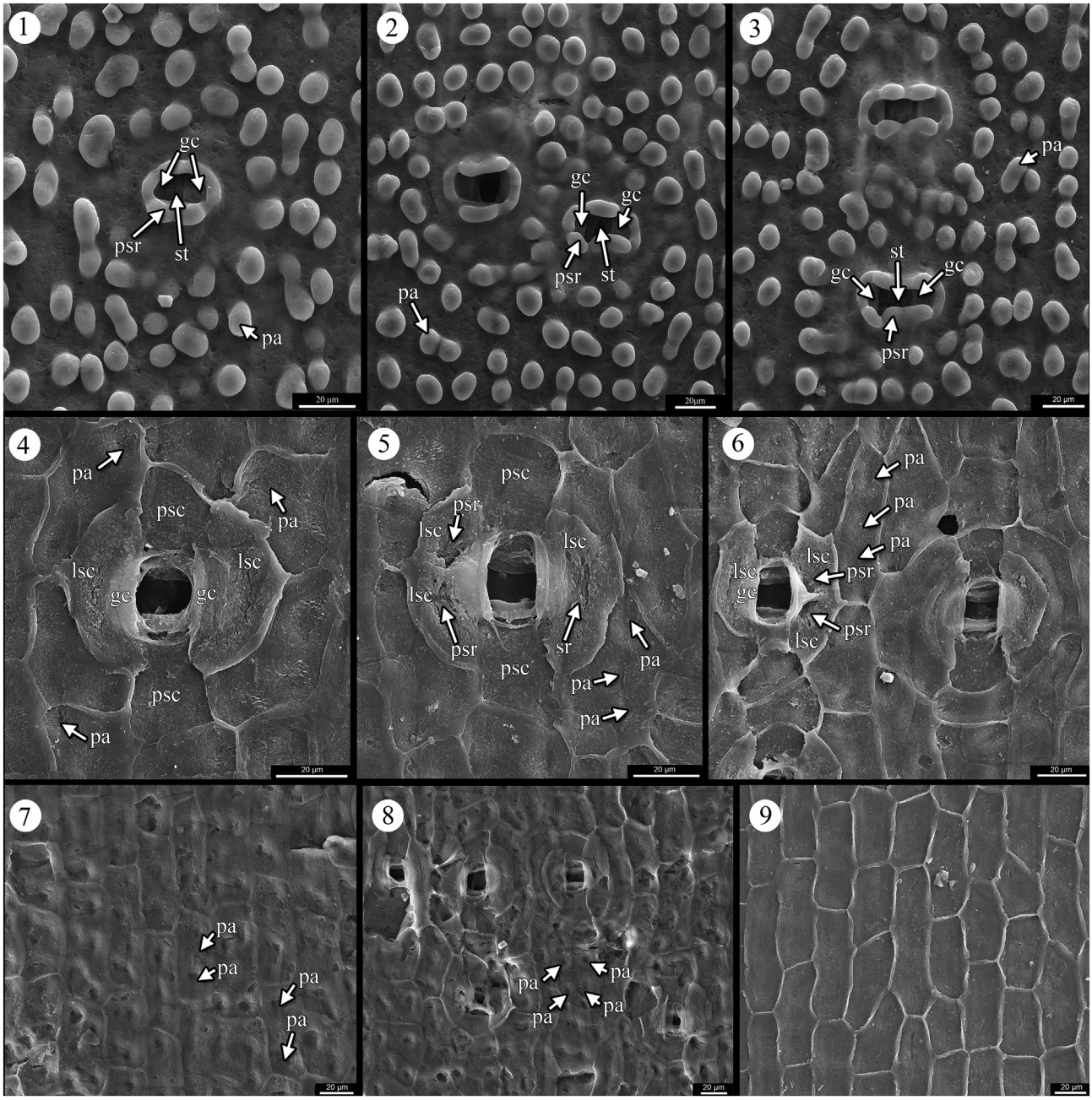

Plate VII. *Taxus huolingolensis* sp. nov., scanning electron micrographs of details of stomatal complexes and epidermal cells from a single fossil leaf. PB23867. **1–3.** Abaxial cuticle outer surface showing details of stomata and epidermal cell outlines; note isodiametric papillae on epidermal cells and transversely elongated papillate rings formed by papillae on subsidiary cells. **4–6.** Abaxial cuticle inner surface showing the shallow cavities on periclinal walls of epidermal cells and deeper cavities on periclinal walls of subsidiary cells; note that the stoma in **4** is surrounded by two elongated lateral subsidiary cells and two polar subsidiary cells, whereas the stoma in **5** is surrounded by three lateral subsidiary cells and two polar subsidiary cells. **7.** Abaxial cuticle inner surface in the papillate submarginal zone showing shallow cavities on periclinal walls. **8.** Abaxial cuticle inner surface of stomatal band showing stomata and epidermal cells; note shallow cavities on epidermal cells and deep cavities on subsidiary cells. **9.** Abaxial cuticle inner surface over the midrib zone showing elongated rectangular epidermal cells; note the periclinal walls of cells are almost smooth. Abbreviations: gc, guard cell; psr, papillate stomatal ring; lsc, lateral subsidiary cell; psc, polar subsidiary cell; pa, papilla; st, stoma. Scale bars = 20 μm.

there are shallow cavities on the inner cuticle surface, suggesting the papillae on the outer surface are more-or-less hollow (Plate VII, 7).

The two stomatal bands are well-defined but not in obvious grooves or depressions on the abaxial leaf surface. They are similar in width and structure, ca. 320–360 μm wide, and extend from the leaf base to the leaf apex. Stomata are rare or absent in the decurrent leaf bases. Epidermal cells in the stomatal zones are similar in size and shape to those of the sub-marginal papillate non-stomatal bands, including the papillae on the periclinal walls (Plate VI, 3, 5, Plate VII, 1–3, 7, 8). Stomata are longitudinally oriented, and arranged in 3–5 short, discontinuous longitudinal rows in each stomatal band (Plate V, 2, Plate VI, 3, 5). Adjacent stomata rows are usually separated by one or two files of epidermal cell outlines (Plate VI, 5). Sometimes two adjacent stomatal complexes are in direct contact, but they do not share lateral subsidiary cells (Plate V, 5, Plate VII, 2, 6). Adjacent stomatal complexes in the same row are commonly separated by one to four epidermal cell outlines (Plate V5, Plate VII, 3, 8).

Stomatal complexes are amphicyclic, ca.75–86 μm long and 47–66 μm wide. Two guard cells are surrounded by the outlines of 2–4 specialized lateral subsidiary cells and two smaller rectangular polar

Table 1
Comparison of leaves of *Taxus huolingolensis* sp. nov. with extant and fossil Taxaceae.

Taxa	Leaf shape	Leaf size (mm)	Stomatal type	Anticlinal walls of epidermal cells	Papillae on epidermal cells on abaxial cuticle
***Taxus huolingolensis* sp. nov.**	Linear	10–20 × 1.0–2.0	Amphicyclic	Straight	2–6 isodiametric protuberances
Taxus spp.	Linear	10–40 × 1.0–3.5	Amphicyclic	Straight	Several isodiametric protuberances
Pseudotaxus chienii	Linear	10–26 × 2.0–4.5	Monocyclic	Straight	Absence
Torreya spp.	Linear to linear-lanceolate	10–70 × 2.0–4.5	Monocyclic	Straight or undulating	Vertically elongated protuberances
Amentotaxus spp.	Lanceolate to linear-lanceolate	30–110 × 5.0–11	Monocyclic	Straight	Absence
Austrotaxus spicata	Narrowly lanceolate	60–170 × 3.5–7.0	Amphicyclic	Straight	Absence
Cephalotaxus spp.	Linear-lanceolate	20–100 × 2.0–7.0	Amphicyclic	Straight	Absence or cuticular thickened
Palaeotaxus rediviva	Linear to linear-lanceolate	12–22 × 1.7–2.3	Amphicyclic	Undulating	Absence
Marskea jurassica	Linear to linear-lanceolate	15–25 × 1.5–2.5	Monocyclic	Wavy to straight	Strong longitudinal ridge or small protuberances
Bartholinodendron punctulatum	Linear or linear-lanceolate	≤15 × 0.7–1.5	Incompletely amphicyclic, monocyclic	Straight to wavy	1–4 short and isodiametric protuberance
Tomharrisia romosa	Narrowly lanceolate to linear	10–38 × 2.0–4.0	Monocyclic	Wavy or undulating	Faint cuticular ridge or strong papillae
***Storgaardia* spp.**	Linear or lanceolate	30–100 × 2.0–12.0	Monocyclic	Straight	Absence or unknown

Note. Fossil taxa are in bold. Data from Florin (1958), Harris (1935, 1976), Fu et al. (1999a, 1999b), Li et al. (2016), Farjon (2017), Elpe et al. (2017).

subsidiary cells (Plate V, 6, 7, Plate VII, 4–6). The guard cells are sunken and kidney-shaped (Plate VII, 1–3). The lateral subsidiary cells are usually ca. 25–55 μm long and 18–25 μm wide, with strongly developed anticlinal walls (Plate VII, 4–6). Polar subsidiary cells are ca. 22–35 μm long and 17–24 μm wide (Plate V, 6, 7, Plate VII, 4–6).

Each subsidiary cell bears one or two papillae on the outer cuticle surface, and the papillae of the same stomatal complex are often slightly fused to form a transversely elongated stomatal ring around the stomatal pit (Plate VII, 1–3). Stomatal pits are oblong or elliptical in outline, ca. 26–29 μm long and 6–10 μm wide (Plate V, 5–7, Plate VII, 1–3). The inner periclinal cuticular surface of the lateral subsidiary cell outlines sometimes have distinct cavities, whereas the cavities on the inner cuticular surface of polar subsidiary cell outlines are shallower (Plate VII, 4–6), indicating the papillae are on the lateral subsidiary cells are partly hollow, whereas they are solid on the polar subsidiary cells.

4. Comparison and discussion

4.1. Generic assignment

The fossil leaves and shoots described here closely resemble those of extant Taxaceae in form, size, and details of cuticular anatomy. Among extant conifers, in addition to Taxaceae, some genera of Pinaceae [*Cathaya* Chun et Kuang, *Tsuga* (Endl.) Carrière, *Pseudotsuga* Carrière, and *Nothotsuga* Hu ex C.N. Page] and taxodiaceous Cupressaceae (*Sequoia* Endlicher, *Metasequoia* Miki ex Hu & Cheng, *Cunninghamia* R. Brown, and *Taxodium* Rich.), also have linear leaves that are dorsiventrally flattened as in the fossils (Fu et al., 1999c; Farjon, 2017). However, the leaves of these extant conifers lack the characteristic prominent, densely spaced papillae seen on the abaxial cuticle of the fossil leaves, which are also seen in extant Taxaceae.

The new fossil leaves from the Gucheng mine are very similar to the leaves of extant Taxaceae, especially those of *Taxus*, and to a lesser extent *Torreya* and *Cephalotaxus*. Leaves of some species of *Cephalotaxus* [*C. mannii* J.D. Hooker, *C. lanceolata* K.M. Feng, *C. sinensis* (Rehder & E.H. Wilson) H.L. Li, *C. fortunei* Hooker] have longitudinal cuticular ridges on the periclinal walls of epidermal cells on the abaxial leaf surface. Leaves of *Torreya* have crowded vertically elongated papillae on the abaxial leaf surface (Table 1; Shi et al., 2010; Farjon, 2017; Elpe et al., 2017). However, the papillae on the abaxial cuticle of the fossil leaves differ in being short and more-or-less isodiametric. Leaves of *Amentotaxus*, *Torreya*, and *Cephalotaxus* have a single well-developed resin canal (Fu et al., 1999a, 1999b; Ghimire et al., 2014; Farjon, 2017), which is not present in the fossil leaves. Leaves of other Taxaceae (*Amentotaxus*, *Austrotaxus*, *Pseudotaxus*), like those of Pinaceae and taxodiaceous Cupressaceae, differ from the fossil leaves in lacking papillae on the abaxial epidermis (Table 1; Fu et al., 1999a; Ghimire et al., 2014; Farjon, 2017; Elpe et al., 2017).

The fossil leaves and leafy shoots from the Gucheng mine are most similar to those of *Taxus*. The key similarities include: (a) linear leaves with long decurrent leaf bases helically arranged on the shoots; (b) leaves lacking resin canals or resin bodies; (c) the abaxial leaf cuticle with well-developed, dense papillae; (d) papillae on the abaxial leaf cuticle short and isodiametric; (e) stomata longitudinally oriented and arranged in short, discontinuous longitudinal rows; (f) stomatal pit surrounded by a papillate stomatal ring formed by papillae on periclinal walls of the subsidiary cells (Plate II, 6–8, Plate VIII, 1–12, Plate IX, 1–9; e.g., Cope, 1998; Fu et al., 1999a; Ghimire et al., 2014; Elpe et al., 2017; Farjon, 2017).

4.2. Comparison with living species of *Taxus*

Among extant species of *Taxus*, *T. baccata* L. (the European yew), the Asian species [*T. chinensis* (Pilg.) Rehd., *T. cuspidata* Siebold & Zucc., *T. mairei* (Lemée & Lév.) S.Y. Hu ex T.S. Liu, *T. wallichiana* Zucc., *T. contorta* Griff.], and *T. canadensis* Marshall and *T. globosa* Schltdl. from North America, all differ from *T. huolingolensis* in having wider leaves (2–4 mm) with more (7–21) stomatal rows in each stomatal band (Plate I, 9–14, Plate IX, 1, 4, 7; Table 2; Möller et al., 2007; Spjut, 2007a, 2007b; Ghimire et al., 2014; Farjon, 2017). Moreover, in most of these extant species, the non-stomatal midrib zone on the abaxial cuticle lacks papillae (Plate IX, 1, 4, 7; Table 2; Elpe et al., 2017). In contrast, the leaves of *T. huolingolensis* are narrower (1.2–2.0 mm) with fewer (3–5) stomatal rows in each stomatal band and have prominent papillae on the non-stomatal midrib zones of the abaxial cuticle.

The extant North American species *T. floridana* Nutt. Ex Chapm. (the Florida yew) resembles *T. huolingolensis* in the size of leaves (Plate I, 15, 16), but differs in having more stomatal rows in each stomatal band (5–7 compared to 3–5 in *T. huolingolensis*) and in lacking papillae over the midrib (Plate VIII, 8–10; Table 2). The North American species, *T. brevifolia* Nutt. (the Pacific yew, Plate I, 17, 18, Plate II, 6; Plate VIII, 1–6), is most similar to *T. huolingolensis* in the form and size of leaves, the papillate midrib zone, and the more-or-less solid papillae on epidermal cells in stomatal bands and the sub-marginal papillate zones (Plate VIII, 3, 5; Table 2; Elpe et al., 2017). However, in *T. brevifolia* the number

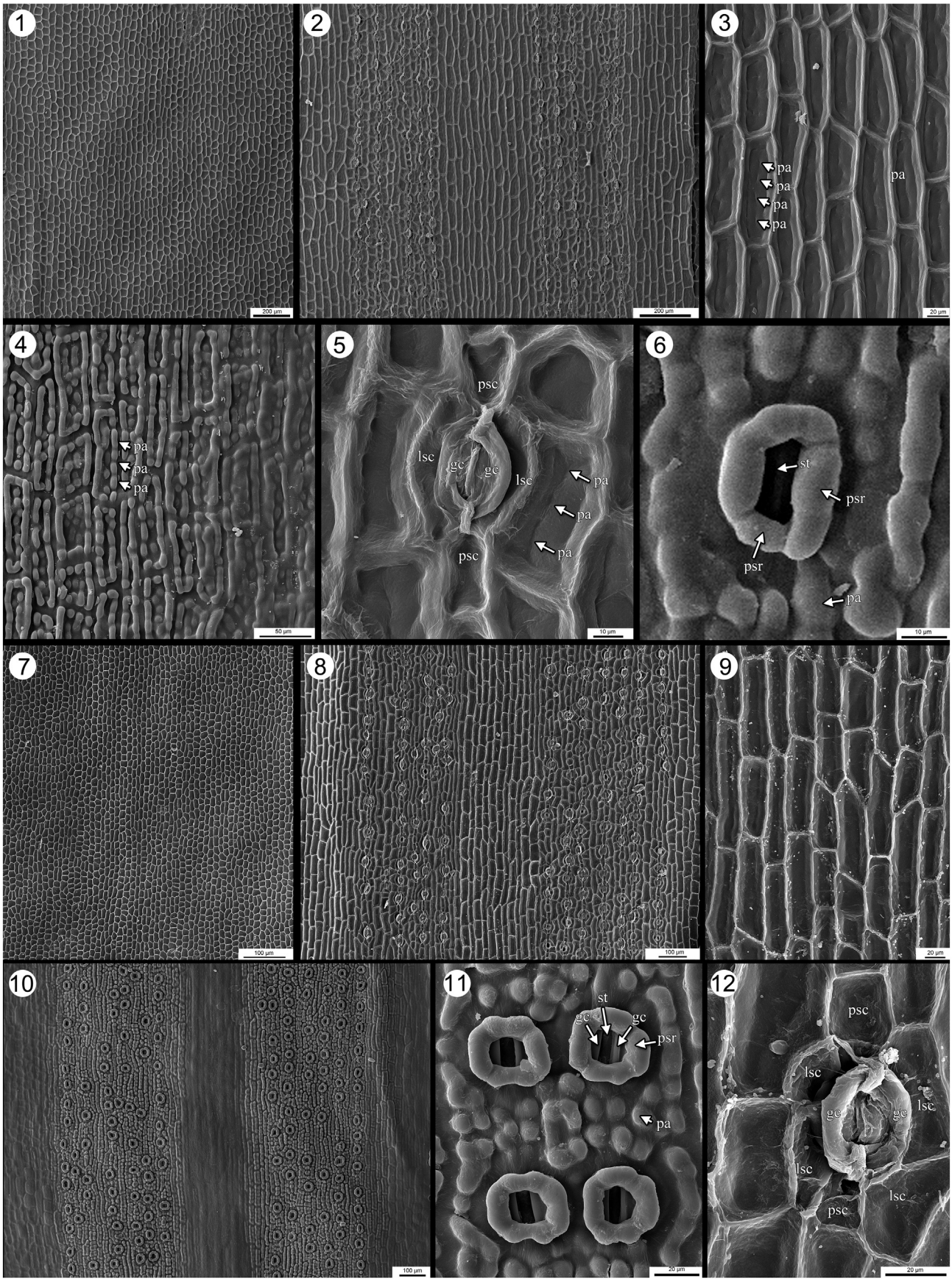
1
200 μm
2
200 μm
3
pa
pa
pa
pa
pa
20 μm
4
pa
pa
pa
50 μm
5
psc
lsc
gc
gc
lsc
pa
pa
psc
pa
10 μm
6
st
psr
psr
pa
10 μm
7
100 μm
8
100 μm
9
20 μm
10
100 μm
11
st
gc
gc
psr
pa
20 μm
12
psc
lsc
gc
gc
lsc
lsc
lsc
psc
20 μm

of stomatal rows in each stomatal band (4–7) is slightly more than that in *T. huolingolensis* (3–5), and papillae are present over nearly the entire abaxial surface of the leaf (Plate VIII, 4). In contrast, *T. huolingolensis* has two narrow marginal zones that lack papillae on the abaxial leaf surface. In addition, the smooth inner surface of the abaxial cuticle indicates that the papillae on non-stomatal midrib zones of abaxial cuticle are solid in *T. huolingolensis*, whereas in *T. brevifolia* the papillae appear to be hollow as indicated by small cavities on the inner cuticle surface (Plate VIII, 3).

4.3. Comparison with other fossil Taxaceae

Especially important for comparison with *Taxus huolingolensis* are *T. acuta* Deng and *T. guyangensis* because both are known from the Early Cretaceous of Inner Mongolia. *Taxus acuta* was described based on compressed leafy shoots from the Early Cretaceous Huolinhe Formation of the Huolinhe Basin in eastern Inner Mongolia (Deng, 1995), whereas *T. guyangensis* was described based on a leafy shoot with attached seed-bearing structures from the Early Cretaceous of Guyang Basin in central Inner Mongolia (Xu et al., 2015).

Leaves of *T. acuta* are similar to those of *T. huolingolensis* in leaf form and phyllotaxis, but they lack the characteristic papillae seen on the abaxial leaf cuticle of our new material and also extant *Taxus* (Table 2; Deng, 1995). *Taxus guyangensis* is also similar to *T. huolingolensis* but lacks papillae in midrib zone and has larger leaves: 18–32 mm long and 2.2–3.2 mm wide, compared to 10–20 mm long, typically 12–16 mm, and ca. 1.2–2.0 mm wide in *T. huolingolensis* (Table 2; Xu et al., 2015).

Also from the Early Cretaceous of Northeast China is *Taxus intermedius* (Hollick) Meng et Chen described based on leafy shoots and a single seed from the Fuxin Basin in western Liaoning Province and Yanbian in eastern Jilin Province (Chen et al., 1988; Zhao, 2009), but its leaf cuticle is poorly preserved, precluding detailed comparison with *T. huolingolensis* (Table 2; Chen et al., 1988). However, leaves of *T. intermedius* are generally wider (more than 2.0 mm) than those of our new material from the Huolinhe Formation.

Several genera of Jurassic and Cretaceous age fossils, including *Marskea jurassica* (Florin) Harris, *Palaeotaxus rediviva* Florin, *Bartholinodendron punctulatum* Florin, *Tomharrisia ramosa* Florin and *Storgaardia spectabilis* Harris have been interpreted as related to Taxaceae (Table 1), and there are also several records of *Taxus* from the Cenozoic of Asia, Europe and North America based on isolated leaves and leafy shoots. None of these fossils are so similar to *Taxus huolingolensis* that they preclude the establishment of the new species, but they are of interest for interpreting the evolution of the family.

Taxus jurassica Florin and *T. harrisii* Florin from the Middle Jurassic of Yorkshire, England were initially assigned to the extant genus because they bear striking resemblance to extant *Taxus* in the apparent helical arrangement of leaves on their leafy shoots (*T. jurassica*), the form and size of individual leaves and structural details of the leaf cuticle (Florin, 1958). However, Harris (1976) later united *T. jurassica*, *T. harrisii*, and *Marskea thomasiana* Florin, which are all from the Lower Deltaic of Yorkshire, into a new combination, *Marskea jurassica* based on close similarities in leaf morphology and cuticular structure. With more detailed studies of shoots after separation of their bases, and shoots bearing several successive pairs of leaves, Harris (1976) also recognized that the leaf phyllotaxis of *M. jurassica* was opposite and decussate, a characteristic feature of extant *Amentotaxus* and *Torreya*, rather than helical as had originally been inferred. Harris (1976) also noted that leaves of *M. jurassica* differ from those of extant *Taxus* in the more-or-less undulating anticlinal flanges that delimit the epidermal cell outlines on the adaxial cuticle, and also in having stomata that are surrounded by a single ring of subsidiary cells (monocyclic). Extant *Amentotaxus* and *Torreya* have monocyclic stomata, whereas in extant *Taxus* stomata are amphicyclic (bicyclic) with the guard cells surrounded by two rings of subsidiary cells (Elpe et al., 2017). Harris (1976) considered *M. jurassica* to exhibit a combination of the characters of extant *Amentotaxus*, *Taxus* and *Torreya*. Recent phylogenetic analysis suggests that *M. jurassica* may be more closely related to *Amentotaxus* than to other genera in the family (Dong et al., 2020).

Marskea jurassica and *Taxus huolingolensis* are similar in the form and size of their leaves and details of their cuticle structure, including the relatively low number of stomatal rows in each stomatal band (3–6 in *M. jurassica,* 3–5 in *T. huolingolensis*), the absence of stomata or papillae on the adaxial cuticle, the presence of dense, prominent papillae, and stomata bearing subsidiary cells with developed rampart-like papillae on the abaxial cuticle, and stomata that are longitudinally oriented and arranged in short, discontinuous longitudinal rows. However, *T. huolingolensis* differs from *M. jurassica* in having helically arranged leaves, amphicyclic stomatal complexes, and epidermal cell outlines with straight, rather than more-or-less undulating, anticlinal walls on the adaxial and abaxial cuticle. In all these features, *T. huolingolensis* is more similar to extant *Taxus* than *M. jurassica.* We therefore assign the fossil leaves from the Gucheng locality to the extant genus, pending additional information on the corresponding reproductive structures.

Palaeotaxus rediviva was described based on leafy shoots with attached seed-bearing structures from the Early Jurassic (Hettangian) of southern Sweden (Florin, 1958) and is currently the earliest reliable fossil record of Taxaceae. *Palaeotaxus rediviva* resembles *Taxus huolingolensis* in the form, size and helical arrangement of leaves on the leafy shoots, but differs in its non-papillate abaxial leaf cuticle.

Bartholinodendron punctulatum [= *Elatocladus punctulatus* (Florin) Harris] known based on isolated leaves from the Middle Jurassic of Denmark and Yorkshire, England (Florin, 1958) is also similar to *T. huolingolensis* and extant *Taxus* in leaf gross morphology and has papillate abaxial cuticles. However, unlike in *T. huolingolensis* the papillae on the periclinal walls of the subsidiary cells do not form a ring surrounding the stomatal pit. Florin assigned the material to a new genus but considered *B. punctulatum* probably closely related to *Taxus* (Florin, 1958).

Tomharrisia ramosa [= *Elatocladus ramosus* (Florin) Harris] from the Middle Jurassic of Yorkshire, England has also been referred to Taxaceae

Plate VIII. Scanning electron micrographs of leaf cuticles and stomata of extant *Taxus* species. **1–6.** *T. brevifolia* Nutt., cuticles from a single leaf. NAS00166219. **1.** Adaxial cuticle inner surface showing polygonal-isodiametric to rectangular epidermal cell outlines arranged in longitudinal files. **2.** Abaxial cuticle inner surface in middle part of leaf across almost the full leaf width showing elongated rectangular epidermal cells and stomata arranged in irregular discontinuous longitudinal files; note that each stomatal band contains 6–7 stomatal rows. **3.** Abaxial cuticle details of epidermal cells on midrib zone, inner cuticle surface showing elongated epidermal cell outlines with well-developed anticlinal walls; note the shallow cavities on the periclinal walls that correspond to the papillae on the external surface. **4.** Abaxial cuticle outer surface near the leaf margin showing scattered isodiametric papillae that are frequently fused into longitudinal rows. **5.** Abaxial cuticle inner surface showing details of elongated lateral subsidiary cells and two polar subsidiary cells; note the shallow cavities epidermal cells and deep cavities on subsidiary cells. **6.** Abaxial cuticle details of stoma on outer surface showing the papillate stomatal ring. **7–12.** *T. floridana* Nutt. ex Champ., cuticles from a single leaf. NAS00166214. **7.** Adaxial cuticle inner surface showing polygonal-isodiametric to rectangular epidermal cell outlines arranged in longitudinal files. **8.** Abaxial cuticle inner surface in middle part of leaf across almost the full leaf width showing elongated rectangular epidermal cell outlines and stomata arranged in irregular discontinuous longitudinal files; note that each stomatal band contains 5–7 stomatal rows. **9.** Abaxial cuticle inner surface over the midrib showing elongated epidermal cell outlines with well-developed anticlinal flanges. **10.** Abaxial cuticle outer surface in middle part of leaf across almost the full leaf width showing papillate stomatal bands, non-papillate midrib, and the marginal zones; note that each stomatal band contains 5–7 irregular discontinuous stomatal rows. **11.** Abaxial cuticle outer surface showing details of stomata and papillate stomatal rings. **12.** Abaxial cuticle showing details of stoma on inner cuticle surface with four lateral subsidiary cells and two polar subsidiary cells. Abbreviations: gc, guard cell; psr, papillate stomatal ring; lsc, lateral subsidiary cell; psc, polar subsidiary cell; pa, papilla; st, stoma. Scale bars: **1, 2** = 200 μm; **3, 9, 11, 12** = 20 μm; **4** = 50 μm; **5, 6** = 10 μm; **7, 8, 10** = 100 μm.

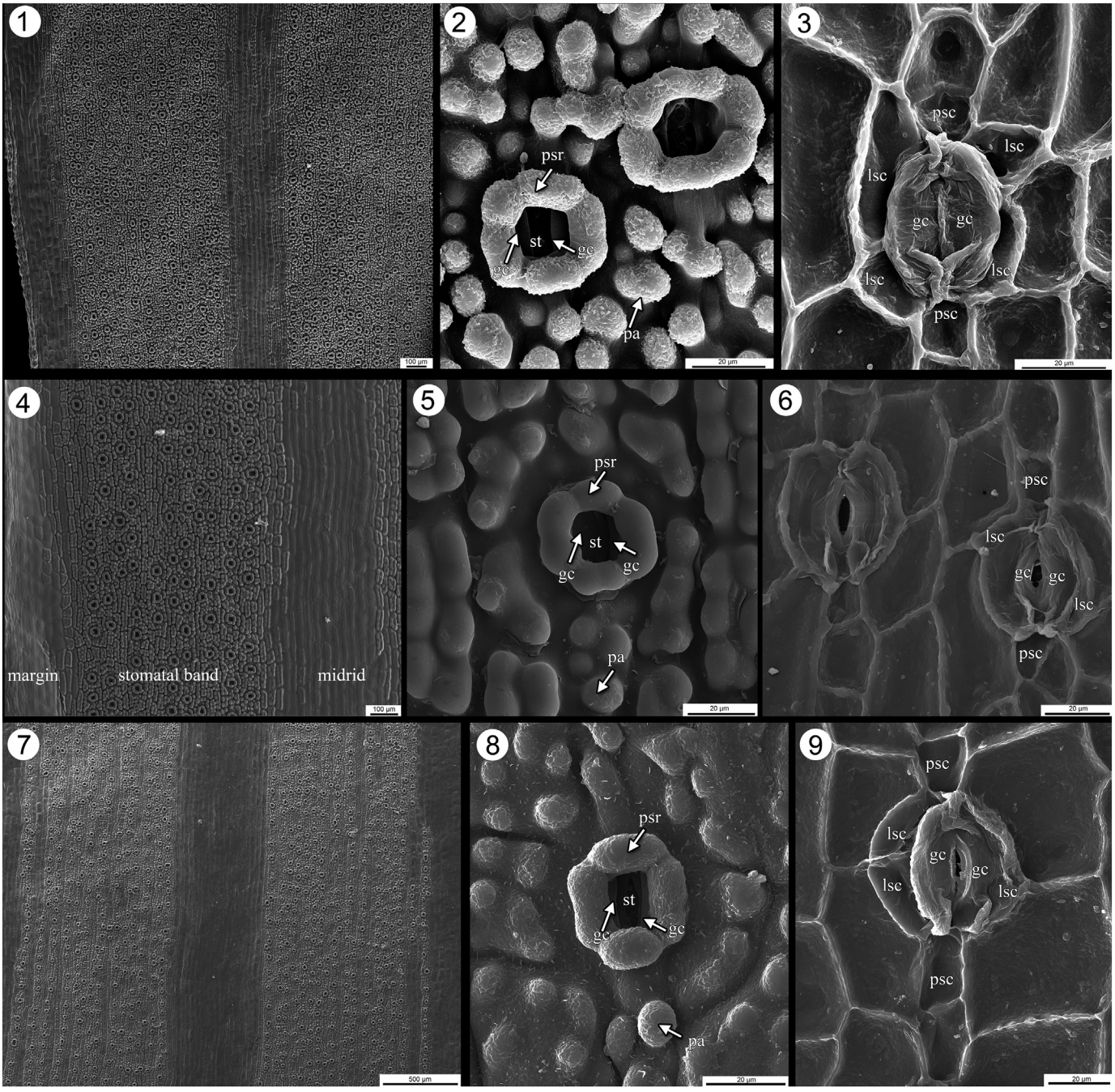

Plate IX. Scanning electron micrographs of abaxial leaf cuticles of extant *Taxus* species. **1–3.** *Taxus wallichiana* Zucc., cuticles from a single leaf. NAS00166100. **1.** Outer surface of cuticle in middle part of leaf with two stomatal bands separated by the midrib, each with large numbers of stomata and well-developed papillae and midrib. Each stomatal band contains 12–14 irregular discontinuous longitudinal files of stomata that are absent from the marginal zones with the epidermal cells also lack papillae. **2.** Detail of outer surface of cuticle showing the papillate stomatal rings. **3.** Detail of inner surface of cuticle showing stomatal complex; note deep cavities on periclinal walls of subsidiary cells. **4–6.** *Taxus chinensis* (Pilg.) Rehd., cuticles from a single leaf. Tree no. 030251 (Chenshan). **4.** Outer surface of cuticle showing papillate stomatal band and non-papillate midrib and marginal zones; note the stomatal band contains 10 irregular discontinuous longitudinal rows of stomata. **5.** Detail of outer surface of cuticle showing the papillate stomatal ring. **6.** Detail of inner surface of cuticle showing two stomatal complexes; note smooth periclinal walls of epidermal cells. **7–9.** *Taxus mairei* (Lemée & Lév.) S.Y. Hu ex T.S. Liu, cuticles from a single leaf. Tree no. 102580 (Chenshan). **7.** Outer surface of cuticle in middle part of leaf showing papillate stomatal bands and non-papillate midrib and marginal zones; note each stomatal band contains 13–16 irregular discontinuous longitudinal files of stomata. **8.** Detail of outer surface of cuticle showing the papillate stomatal ring. **9.** Detail of inner surface of cuticle showing smooth periclinal walls of epidermal cell outlines. Abbreviations: gc, guard cell; psr, papillate stomatal ring; lsc, lateral subsidiary cell; psc, polar subsidiary cell; pa, papilla; st, stoma. Scale bars: **1** = 200 μm; **4** = 100 μm; **7** = 500 μm; **2, 3, 5, 6, 8, 9** = 20 μm.

(Florin, 1958; Harris, 1976), but differs from *T. huolingolensis*, and most other fossil taxads, in having toothed leaves that are oppositely to subopositely arranged. Epidermal cells in the non-stomatal zones of abaxial cuticle are also non-papillate and the anticlinal flanges of the epidermal cell outlines are distinctly undulating (Florin, 1958; Harris, 1976).

Storgaardia Harris, described based on leafy shoots from the earliest Jurassic of East Greenland, is thought to combine features of several extant genera of Taxaceae (Harris, 1935; Florin, 1958). Like *T. huolingolensis*, *S. spectabilis* has a papillate stomatal ring surrounding the stomatal pit, but differs in having larger, lanceolate leaves,

Table 2
Comparison of leaves of *Taxus huolingolensis* sp. nov. with living and fossil species of *Taxus* in leaf morphology and cuticular structure.

Taxon	Leaf length (cm)	Leaf width (mm)	Number of stomata rows within band	Papillae on midribs	Nature of papillae	Age	Distribution
***Taxus huolingolensis* sp. nov.**	1.0–2.2	1.2–2.0	3–5	Present	Solid	Early Cretaceous	NE China
T. baccata	1.0–3.5	2.0–2.5	8–10	Absent	Solid	Extant	Europe, N Africa, W Asia
T. cuspidata	1.5–3.0	2.2–3.5	7–21	Absent	Hollow	Extant	E Asia
T. contorta	1.5–4.0	1.5–2.5	7–8	Absent	Solid	Extant	E Asia
T. chinensis	1.5–2.0	2.0–3.2	11–17	Absent	Solid	Extant	E Asia
T. mairei	1.5–3.5	2.0–4.0	11–16	Absent	Solid	Extant	E Asia
T. wallichiana	1.5–3.5	2.0–4.0	12–15	Present	Hollow	Extant	E, SE Asia
T. canadensis	1.0–2.0	2.2–3.5	7–9	Absent	Solid	Extant	N America
T. globosa	2.0–3.0	2.0–2.5	8–11	Present	Hollow	Extant	N America
T. floridana	1.5–2.5	1.0–2.0	5–7	Absent	Solid	Extant	N America
T. brevifolia	1.0–2.0	1.5–3.0	4–7	Present	Solid	Extant	N America
T. guyangensis	1.8–3.2	2.2–3.2	4–5	Absent	?	Early Cretaceous	N China
T. acuta	1.0–1.5	1.0–2.0	8–9	Absent	?	Early Cretaceous	NE China
T. intermedius	1.5–2.7	2.0–3.0	?	?	?	Early Cretaceous	NE China
T. engelhardtii	0.8–1.4	1.5–2.5	7–10	Present	?	Oligocene, early Miocene	Central Europe
T. schornii	2.0–2.5	3.0	8–9	Present	?	Middle Miocene	NW USA
T. qinghaiensis	2.0–2.5	1.5–2	?	?	?	Middle Miocene	NW China
***T. inopiunata* (*Taxus* sp. aff. *baccata*)**	1.9	1.8	?	?	?	Late Miocene	SE Europe
***Taxus* sp.1**	10 (part.)	2	9	Absent	?	Early Miocene	Central Europe
***Taxus* sp. 2**	4 (part.)	2	4	Absent	?	Late Pliocene	Central Europe

Note. Fossil species are in bold. Data of extant species from Spjut (2007a, 2007b), Elpe et al. (2017) and Farjon (2017), and fossil data respectively from the present study, Guo (1980), Kvaček (1976, 1984), Chen et al. (1988), Deng (1995), Kvaček and Rember (2000, 2007), Macovei (2013), and Xu et al. (2015).

monocyclic stomata and non-papillate abaxial midrib (Florin, 1958; Harris, 1976; Li et al., 2016).

Taxus leaves are also known from the Cenozoic of Asia, Europe and North America (Kvaček, 1976, 1984; Guo, 1980; Kvaček and Rember, 2000, 2007; Kunzmann and Mai, 2005; Macovei, 2013), but in most cases the cuticles of these fossils are unknown or poorly understood. For example, this is the case for *T. qinghaiensis* Guo from the middle Miocene of Zeku, Qinghai Province, Northwest China (Guo, 1980) and *T. inopiunata* (= *Taxus* sp. aff. *baccata*) from the late Miocene of Romania (Macovei, 2013).

Among the *Taxus* leaves described from the Cenozoic, *T. engelhardtii* Kvaček from the Oligocene and early Miocene of central Europe is most similar to *T. huolingolensis* in the form and size of leaves, papillate midrib and sub-marginal non-stomatal zones, but differs in having more stomatal rows (7–10) in each stomatal band (Table 2; Kvaček, 1976, 1984; Kunzmann and Mai, 2005). Also similar are *Taxus* sp.1 and *Taxus* sp. 2 known from leaf fragments from the early Miocene and the late Pliocene of the Cheb Basin, central Europe respectively (Kvaček, 1984). However, both can be distinguished from *T. huolingolensis* by the abaxial cuticle over the midrib lacking papillae (Table 2). *Taxus schornii* Kvaček et Rember from middle Miocene of northern Idaho, northwest USA, described based on isolated linear leaves with well-preserved cuticles (Kvaček and Rember, 2000, 2007) does have conspicuous papillae on midrib zone of the abaxial cuticle, but differs from *T. huolingolensis* in having wider leaves (3.0 mm) with more stomatal rows (8–9) in each stomatal band (Table 2).

4.4. Evolutionary implications

Well-preserved fossils of Taxaceae with vegetative shoots and reproductive structures attached are very rare. However, diverse leaves and leafy shoots, and also woods, that are clearly referable to Taxaceae based on gross morphology and details of cuticle structure, are known from the Jurassic onwards (Florin, 1958; Harris, 1976; Philippe et al., 2019). Together these fossils demonstrate the diversity of the family in the later Mesozoic, but all of these fossils (e.g., *Marskea jurassica*) exhibit characters of several extant genera of Taxaceae, and thus cannot be referred to any extant genus.

The only convincing early fossil record of *Taxus* based on leafy shoots with an attached seed-bearing structure is *Taxus guyangensis* from the Early Cretaceous of central Inner Mongolia, northern China (Xu et al., 2015). This record is now supplemented by *T. huolingolensis* from the Early Cretaceous of eastern Inner Mongolia, which although unknown from reproductive structures has leaves that bear an especially striking resemblance to leaves of extant *Taxus* in almost every respect, including details of cuticular and stomatal structures (Plates VII, IX). Together, *Taxus huolingolensis* and *T. guyangensis* suggest that among the diverse Taxaceae of the Mesozoic, plants very similar to living *Taxus* were present by the Early Cretaceous and were apparently represented by more than one species. This conclusion needs to be tested by the discovery and description of additional corresponding reproductive material. It is also interesting that among extant species of *Taxus*, both *T. huolingolensis* and *T. guyangensis* are most comparable to the western North American species *T. brevifolia* (Xu et al., 2015). Phylogenetic analyses based on molecular (Leslie et al., 2012) and morphological data (Elpe et al., 2017) both resolve *T. brevifolia* as sister to all other extant *Taxus* species.

A feature of *Taxus huolingolensis* and *T. guyangensis*, in which they differ from most extant species of *Taxus*, is in having narrower stomatal bands with fewer stomatal rows in each band (3–5). The numbers of stomatal rows in each stomatal band are 7–21 in most extant species, but 4–7 in *T. brevifolia* and *T. floridana*. The same phenomenon also occurs in other fossils assigned to the Taxaceae sensu *lato*. For instance, early representatives of *Cephalotaxus*, *C. cretacea* Samylina (Samylina, 1963) and *C. ussuriensis* Krassilov (Krassilov, 1967) from the Early Cretaceous of the Russian Far East, also have fewer stomatal rows in each stomatal band than in extant species of *Cephalotaxus* (Shi et al., 2010). This pattern deserves more detailed consideration given the possibility that the increase in the number of stomatal rows in each stomatal band in *Taxus* and *Cephalotaxus* since the Cretaceous may be related to decreasing concentrations of atmospheric carbon dioxide during Cenozoic.

Declaration of Competing Interest

The authors declare that they have no known competing financial interests or personal relationships that could have appeared to influence the work reported in this paper.

Acknowledgements

The authors thank Qijia Li, Hui Jiang, and Dawei Lu for assistance with fieldwork in the Huolinhe Basin, eastern Inner Mongolia, China; and the Herbarium of Institute of Botany, Jiangsu Province and Chinese Academy of Sciences, and Shanghai Chenshan Botanical Garden for

providing access to extant material of *Taxus*. Funding for this work was supported by the National Science Foundation of China (42172030, 41802014, 41790454, 41688103), the US National Science Foundation grant DEB-1748286, the Strategic Priority Research Program (B) of the Chinese Academy of Sciences (XDB2600000) and the Oak Spring Garden Foundation.

References

Chen, F., Deng, S.H., 1990. Three species of *Athrotaxites* – Early Cretaceous conifer. Geosci. 4, 27–37 (in Chinese with English abstract).
Chen, F., Meng, X.Y., Ren, S.Q., Wu, C.L., 1988. The Early Cretaceous Flora and Coal-Bearing Strata of Fuxin Basin and Tiefa Basin, Liaoning Province. Geological Publishing, Beijing (in Chinese and English).
Cheng, Y.C., Nicolson, R.G., Tripp, K., Chow, S.M., 2000. Phylogeny of Taxaceae and Cephalotaxaceae genera inferred from chloroplast *matK* gene and nuclear *r*DNA ITS region. Mol. Phylogenet. Evol. 14, 353–365.
Christenhusz, M.J.M., Revel, J.L., Farjon, A., Gardner, M.F., Mill, R.R., Chase, M.W., 2011. A new classification and linear sequence of extant gymnosperms. Phytotaxa 19, 55–70.
Cope, E., 1998. Taxaceae: the general and cultivated species. Bot. Rev. 64, 291–322.
Deng, S.H., 1991. Early Cretaceous fossil plants from Huolinhe Basin in Inner Mongolia. Geosci. 5, 147–156 (in Chinese with English abstract).
Deng, S.H., 1995. Early Cretaceous Flora of Huolinhe Basin, Inner Mongolia, Northeast China. Geological Publishing House, Beijing.
Dong, M., Sun, G., 2012. *Ginkgo huolinheensis* sp. nov. from the Lower Cretaceous of Huolinhe Coal Field, Inner Mongolia, China. Acta Geol. Sin. (Engl. Ed.) 86, 11–19.
Dong, C., Shi, G.L., Herrera, F., Wang, Y.D., Herendenn, P.S., Crane, P.R., 2020. Middle-Late Jurassic fossils from northeastern China reveal morphological stasis in the catkin-yew. Natl. Sci. Rev. 7, 1765–1767.
Eckenwalder, J.E., 2009. Conifers of the World. Timber Press, Portland, Oregon, USA.
Elpe, C., Knopf, P., Stützel, T., Schulz, C., 2017. Cuticle micromorphology and the evolution of characters in leaves of Taxaceae *s. l.* Bot. J. Linn. Soc. 184, 503–517.
Farjon, A., 2017. A Handbook of the world's Conifers. Second, revised edition. Volume 1. Brill, Leiden-Boston.
Ferguson, D.K., 1978. Some current research on fossil and recent taxads. Rev. Palaeobot. Palynol. 26, 213–226.
Florin, R., 1958. On Jurassic taxads and conifers from north-western Europe and eastern Greenland. Acta Harti. Bergiania. 17, 257–402.
Fu, L.G., Li, N., Mill, R.R., 1999a. Taxaceae. In: Wu, Z.Y., Raven, P.H. (Eds.), Flora of China. Science Press, Beijing and Missouri Botanical Garden Press, St. Louis.
Fu, L.G., Li, N., Mill, R.R., 1999b. Cephalotaxaceae. In: Wu, Z.Y., Raven, P.H. (Eds.), Flora of China. Science Press, Beijing and Missouri Botanical Garden Press, St. Louis.
Fu, L.G., Li, N., Mill, R.R., 1999c. Taxodiaceae. In: Wu, Z.Y., Raven, P.H. (Eds.), Flora of China. Science Press, Beijing and Missouri Botanical Garden Press, St. Louis.
Ghimire, B., Lee, C., Heo, K., 2014. Leaf anatomy and its implications for phylogenetic relationships in Taxaceae *s. l.* J. Plant Res. 127, 373–388.
Ghimire, B., Lee, C., Heo, K., 2015. Comparative wood anatomy of Taxaceae. Austr. Syst. Bot. 28, 160–172.
Guignard, G., Yang, X.J., Wang, Y.D., 2019. Cuticle ultrastructure of *Baiera furcata* from Northeast China and its implication in taxonomy and paleoenvironment. Rev. Palaeobot. Palynol. 268, 95–108.
Guo, S.X., 1980. Miocene Flora in Zekog County of Qinghai. Acta Palaeontol. Sin. 19, 406–412 (in Chinese with English abstract).
Guo, C., 1995. Sporopollen from the Lower part of the Huolinhe Formation, Huolinhe Basin, Inner Mongolia and its significance. PED 22, 37–44 (in Chinese with English abstract).
Harris, T.M., 1935. The fossil flora of Scoresby Sound, East Greenland. Part 4: Ginkgoales, Coniferales, Lycopodiales and isolated fructifications. Meddelelser om Gronland 112.
Harris, T.M., 1976. The Yorkshire Jurassic Flora, V. Coniferales. British Museum Natural History, London.
Hart, J.A., 1987. A cladistic analysis of conifers: preliminary results. J. Arnold Arbor. 68, 269–307.
Herrera, F., Testo, W.L., Field, A.F., Clark, E.G., Herendeen, P.S., Crane, P.R., Shi, G.L., 2022. A permineralized Early Cretaceous lycopsid from China and the evolution of crown clubmosses. New Phytol In press.
Krassilov, V.A., 1967. Early Cretaceous Flora of South Primorye and its Stratigraphic Significance. Nauka, Moscow (in Russian).
Kunzmann, L., Mai, H.D., 2005. Conifers of the Mastixioideae-flora-from Wiesa near Kamenz (Saxony, Miocene). Palaeontogr. Abt. B 272, 67–135.
Kvaček, Z., 1976. Towards nomenclatural stability of European Tertiary conifers. Neues Jahrb. Geol. P-M 284–300.
Kvaček, Z., 1984. Tertiary taxads of NW Bohemia. Acta Univ. Carol. Geol. 1982 (4), 471–491.
Kvaček, Z., Rember, W.C., 2000. Shared Miocene conifers of the Clarkia flora and Europe. Acta Univ. Carol. Geol. 44, 75–85.
Kvaček, Z., Rember, W.C., 2007. *Calocedrus robustitor* (Cupressaceae) and *Taxus schornii* (Taxaceae): two new conifers from the middle Miocene Latah Formation of northern Idaho. Paleobios 27, 68–79.
Leslie, A.B., Beulieu, J.M., Rai, H.S., Crane, P.R., Donoghue, M.J., Mathews, S., 2012. Hemisphere-scale differences in conifer evolutionary dynamics. Proc. Natl. Acad. Sci. USA 109, 16217–16221.
Li, S.T., Huang, J.F., Yang, S.G., Zhang, X.M., Cheng, S.T., Zhao, G.R., Li, D.N., Li, G.L., Ding, J.L., 1982. Depositional and structural history of the late Mesozoic Huolinhe Basin and its characteristics of coal accumulation. Acta Geol. Sin. 3, 244–254 (in Chinese with English abstract).
Li, Q.J., An, P.C., Li, J., Zhao, Z.R., Wu, J.Y., Wang, Y.D., Zhu, Y.T., Ding, S.T., 2016. Cuticular structure of *Storgaardia* Harris from the Middle Jurassic of Northwest China and its systematic and biogeographical significances. Palaeoworld 26, 149–158.
Macovei, G., 2013. A revision of Taxaceae remains of the late Miocene fossil flora from Chiuzbaia, Maramures county, Romania. Carpath. J. Earth Env. 8, 245–248.
Matsunaga, K.K.S., Herendeen, P.S., Herrera, F., Ichinnorov, N., Crane, P.R., Shi, G.L., 2021. Ovulate cones of *Schizolepidopsis ediae* sp. nov. provide insights into the evolution of Pinaceae. Int. J. Plant Sci. 182, 490–507.
Möller, M., Gao, L.M., Mill, R.R., Li, D., Hollingsworth, M.L., Gibby, M., 2007. Morphometric analysis of the *Taxus wallichiana* complex (Taxaceae) based on herbarium material. Bot. J. Linn. Soc. 155, 307–335.
Philippe, M., Afonin, M., Delzon, S., Jordan, G.J., Terada, K., Thiébaut, M., 2019. A paleobiogeographical scenario for the Taxaceae based on a revised fossil wood record and embolism resistance. Rev. Palaeobot. Palynol. 263, 147–158.
Price, R.A., 1990. The genera of Taxaceae in the southeastern United States. J. Arnold Arbor. 71, 69–91.
Price, R.A., 2003. Generic and familial relationships of the Taxaceae from *rbcL* and *matK* sequence comparisons. Acta Hortic. 615, 235–237.
Ran, J.H., Shen, T.T., Wang, M.M., Wang, X.Q., 2018. Phylogenomics resolves the deep phylogeny of seed plants and indicates partial convergent or homoplastic evolution between Gnetales and angiosperms. Proc. R. Soc. B 285, 20181012.
Samylina, V.A., 1963. The Mesozoic flora of the lower course of the Aldan River. Trans. Bot. Inst. Acad. Sci. USSR. Ser. VIII Palaeobot. 4, 57–140.
Shi, G.L., Zhou, Z.Y., Xie, Z.M., 2010. A new *Cephalotaxus* and associated epiphyllous fungi from the Oligocene of Guangxi, South China. Rev. Palaeobot. Palynol. 161, 179–195.
Shi, G., Herrera, F., Herendeen, P.S., Elizabeth, G.C., Crane, P.R., 2021a. Mesozoic cupules and the origin of the angiosperm second integument. Nature 594, 223–226.
Shi, G.L., Li, J.G., Tan, T., Dong, C., Li, Q.L., Wu, Q., Zhang, B.L., Yin, S.X., Herrera, F., Herendeen, P.S., Crane, P.R., 2021b. Age of the Huolinhe Formation in the Huolinhe Basin, eastern Inner Mongolia, China: evidence from U-Pb zircon dating and palynological assemblages. J. Stratigr. 45, 69–81.
Spjut, R.W., 2007a. A phytogeographical analysis of *Taxus* (Taxaceae) based on leaf anatomical characters. J. Bot. Res. Inst. Texas 23, 291–332.
Spjut, R.W., 2007b. Taxonomy and nomenclature of *Taxus* (Taxaceae). J. Bot. Res. Inst. Texas 23, 201–289.
Sun, G., 1987. *Phoenicopsis* from NE China with discussion on its taxonomy. Acta Palaeontol. Sin. 26, 682–688.
Sun, G., 1993. *Ginkgo coriacea* Florin from Lower Cretaceous of Huolinhe, northeastern Nei Monggol, China. Palaeontogr. Abt. B 230, 159–168.
Sun, G., Shang, P., 1988. A brief report on preliminary research of Huolinhe coal-bearing Jurassic-Cretaceous plants and strata from eastern Inner Mongolia, China. J. Fuxin Min. Inst. 7, 69–76 (in Chinese with English abstract).
Sun, G., Lydon, S.J., Watson, J., 2003. *Sphenobaiera ikorfatensis* (Seward) Florin from the Lower Cretaceous of Huolinhe, eastern Inner Mongolia, China. Palaeontology 46, 423–430.
Wang, X.Q., Ran, J.H., 2014. Evolution and biogeography of gymnosperms. Mol. Phylogenet. Evo. 75, 24–40.
Xu, X.H., Li, R.Y., Dong, C., Wang, Q.J., Jin, P.H., Sun, B.N., 2013. New *Schizolepis* fossils from the Early Cretaceous in Inner Mongolia, China and its phylogenetic position. Acta Geol. Sin. (Engl. Edn.) 87, 1250–1263.
Xu, X.H., Sun, B.N., Yan, D.F., Wang, J., Dong, C., 2015. A *Taxus* leafy branch with attached ovules from Lower Cretaceous of Inner Mongolia, North China. Cretaceous Res. 54, 266–282.
Xu, X.H., Yang, L.Y., Sun, B.N., Wang, Y.D., Chen, P., 2017. A new Early Cretaceous *Ginkgo* ovulate organ with associated leaves from Inner Mongolia, China and its evolutionary significance. Rev. Palaeobot. Palynol. 244, 163–181.
Zhao, G.W., 2009. Conifers from the Lower Cretaceous Changcai Formation in the Yanbian Area, Jilin Province.. Ph. M thesisJilin University, Jilin, China.